香港天文台
HONG KONG OBSERVATORY

Reprint 896

LIDAR Data Analysis for a Tornado on 6 September 2004 at the Hong Kong International Airport

P.W. Chan & Frank Yu*

International Symposium for the Advancement of Boundary Layer Remote Sensing 2010, 28 - 30 June 2010, Saint-Quentin-en-Yvelines, France

*Department of Environment and Conservation, Australia

LIDAR Data Analysis for a Tornado on 6 September 2004 at the Hong Kong International Airport

P.W. Chan[1], Frank Yu[2]

[1]Hong Kong Observatory, 134A Nathan Road, Kowloon, Hong Kong, China, pwchan@hko.gov.hk
[2]Department of Environment and Conservation, Australia

ABSTRACT

A number of tornadoes appeared along a gust front at the Hong Kong International Airport on 6 September 2004, causing injury to a ground personnel and damages to an aircraft. The evolution of the tornadoes was well captured by a Doppler LIght Detection And Ranging (LIDAR) system at the airport. This paper documents the meteorological background and the LIDAR observations of the tornadoes. A more in-depth analysis of the dynamic field associated with a tornado in the event is carried out using 4-dimensional variational method (4DVAR) based on consecutive conical scans of the LIDAR. It turns out that the 4DVAR-analyzed wind field successfully captures the anticyclonic nature of the tornado and the structure of the wind field in its vicinity. The 4DVAR analysis (with a horizontal resolution of 100 m) also shows a number of features of the tornado: (a) a downdraft near the centre of the tornado with a "ring" of updraft around it, though the vertical velocity is generally rather small (~3 m/s); (b) there appears to be a vertical circulation around the tornado, with upward motion to its south and downward motion to its north, which may be one source of vorticity for the formation of the gustnado, and (c) the pressure deficit near the centre of the tornado is ~5 hPa. The analysis has been repeated with higher spatial resolution (e.g. 50 m) in an attempt to analyze the tornado in more detail, but the maximum horizontal wind associated with the tornado does not change significantly. Further study of the formation of the gustnado would be required, e.g. using radar data.

1. INTRODUCTION

At about 5:55 p.m., 6 September 2004 (Hong Kong time = UTC + 8 hours), a small-scale tornado affected the Hong Kong International Airport (HKIA) for several minutes, occurring at about 1.5 – 2 kilometres to the south of the Air Traffic Control Tower and the Doppler Light Detection And Ranging (LIDAR) system. It swept across the cargo apron of the airport and one airline staff was injured. A number of aircraft and ground facilities were damaged. Pallets each weighted about a tonne were moved. One of them was even blown onto the roof canopy of a building by the violent winds. Based on the damages, the tornado belongs to F0 on the Fujita scale.

It was not raining during the occurrence of the tornado. As a result, the Doppler LIDAR provided radial velocity of good quality in capturing the generation, movement and dissipation of the tornado. An analysis of the tornado is presented in this paper based on the LIDAR data. This study mainly focuses on the climax of the event, namely, when the tornado achieved the maximum strength and swept across the apron of HKIA. The 3D wind field and pressure perturbation associated with the tornado would be obtained using four dimensional variational (4DVAR) analysis as applied to the radial velocity provided by the LIDAR.

2. BACKGROUND OF THE EVENT

On 6 September 2004, a trough of low pressure associated with Typhoon Songda affected the coast of southern China. Troughing flow could be analyzed on the surface up to 850 hPa level (not shown). In the upper troposphere (e.g. 200 hPa level), divergence could be analyzed in the region in association with a broad anticyclone (not shown). The atmosphere was humid and unstable as revealed in the radiosonde data on that day. The K index was 35 at 8 a.m. and rose to 41 at 8 p.m. Under the unstable atmosphere, intense convective development was triggered over inland areas of southern China due to solar heating during the day and the thunderstorms so produced moved south towards the coast in the evening.

Starting from about 4 p.m. on that day, the radarscope of Hong Kong showed that there were isolated thunderstorms along the south China coast. Among them, one storm appeared to the west of HKIA at about 5:30 p.m. and brought westerly winds to the western part of the airport. The westerly was basically rain-free and appeared to be the gust front associated with the thunderstorm. It spread eastwards and converged with the background east to southeasterly winds over the eastern part of HKIA. The tornado developed over the convergence zone of the two airstreams.

3. LIDAR AND 4DVAR ANALYSIS

Since the gust front discussed in Section 2 above was free of rain, it was well captured by the LIDAR near the centre of HKIA. In 2004, there was only one LIDAR working at the airport. It uses an infrared laser beam with a wavelength of 2 microns to track the movement of aerosols suspending in the air and thus measure the line-of-sight velocity of the wind. The radial resolution is about 100 m and the maximum measurable range is around 10 km. In September 2004, the LIDAR was configured to make Plan Position Indicator (PPI) scans at elevation angles of 0, 1 and 4.5 degrees as well as Range Height Indicator (RHI) scans with an azimuth angle of 258 degrees with respect to the North. The radial velocity data obtained from all these scans are used in the 4DVAR analysis.

Technical details of the 4DVAR analysis of LIDAR data could be found in Yu and Chan (2009). The cost function used in the present analysis is given as follows:

$$J = Jr + Jd + Js \quad (1)$$

The first term in Eq, (1), Jr , is the difference between forward model predicted radial velocity and the LIDAR

observations within the specified time window (~3 minutes in the present study). Jd is the divergence penalty term used for suppressing the divergence in the initial field. Js is the smoothing penalty term and it helps to smooth the output for easily identifying any possible eddy structures in the retrieved wind field. The governing equations are the Boussineq equations for a shallow atmospheric boundary layer.

4. ANALYSIS RESULTS AT 100 M RESOLUTION

The LIDAR's 1-degree PPI scan image at the climax of the tornado (about 09:54 UTC, 6 September 2004) is shown in Figure 1. The tornado under study is encircled in red. It could be found in the southern side of HKIA at which the cargo apron is located. As a start, 4DVAR analysis is carried out with a horizontal resolution comparable with the radial resolution of the LIDAR, viz. 100 m.

Figures 2 and 3 show the 4DVAR-analyzed horizontal wind vectors (as arrows) and perturbation horizontal velocities (u - <u> and v - <v>, in colour contours) at a height of 200 m above sea level. The anticyclonic flow associated with the tornado is captured successfully by the 4DVAR-retrieved wind field. The perturbation horizontal velocities also show a couple of features:

(a) From the plot of u - <u>, the perturbed easterly wind at the southern part of the tornado is generally stronger than the perturbed westerly wind at the northern part of the system. The former reaches about 8 m/s. Similarly, from the plot of v - <v>, the perturbed northerly wind at the eastern part of the tornado is generally stronger than the perturbed southerly wind at the western part of the system. The former reaches about 10 m/s.

(b) A series of small-scale cyclones and anticyclones (each with a size of several hundred metres) is analyzed at the convergence zone between the westerly flow associated with the gust front and the background east to southeasterly flow at the eastern part of HKIA.

(c) Even with the mean wind subtracted, the perturbed v-component still shows the southerly jet emerging from a gap of Lantau Island at the lower right corner of the analysis domain (Figure 3).

Apart from the horizontal winds, the 4DVAR analysis gives the vertical velocity and the pressure, which are not measured directly by the LIDAR. The perturbation vertical velocity is shown in Figure 4. In general, downward motion up to about -3 m/s is analyzed for the westerly wind over the airport island. At the same time, at the eastern and southern edges of the westerly flow, there are areas of upward motion with a vertical velocity of +3 m/s. As such, there is vertical circulation along the periphery of the gust front. The circulation may be tilted to give rise to a tornado. This is one possibility for the occurrence of the gustnado.

Moreover, as revealed from 4DVAR analysis (Figure 4), the tornado itself has rather complicated pattern of vertical velocity. There is upward motion at its core. At the eastern and western sides of the core, the motion is generally downward. An area of significant upward motion (with vertical velocity of +3m/s) is also identified to the northeast of the core. The origin of this upward motion is not certain, and it may be a perturbation in the vertical circulation associated with the southern periphery of the gust front as discussed earlier in this Section.

The perturbation pressure is shown in Figure 5. At the location of the tornado, there is a perturbed pressure of about -5 hPa. At the same time, to the northeast of the tornado, an area of pressure rise of +3 hPa is identified. A vertical cross section of the core of pressure deficit is shown in Figure 6. It could be seen that the pressure drop occurs over a height up to about 500 m above sea level.

Vertical cross sections of the wind field are shown in Figures 7 to 8. It could be seen that, for the north-south cross sections, the prominent feature is the vertical circulation across the gust front as discussed earlier in the Section. In Figure 7, apart from this vertical circulation, the divergent flow near the ground in association with the northerly wind at the eastern part of the tornado could also be seen. For the east-west cross sections, apart from downward motion in the first few hundred metres above sea level (areas in which w - <w> is coloured blue), there are no prominent features in the vertical circulation.

5. ANALYSIS RESULTS AT 50 M RESOLUTION

In order to study the sensitivity of the 4DVAR analysis results to the horizontal resolution of the analysis grid, another analysis has been carried out with a horizontal resolution of 50 m. The results turn out to be not so satisfactory. As an illustration, the perturbed wind field at a height of 200 m and the perturbed pressure in a vertical cross section near the tornado's core are shown in Figures 9 and 10 respectively. The wind velocities are found to be much weaker than those in the 100-m analysis (c.f. Figure 4) – not only the horizontal velocities, but also for the vertical velocity as well. The pressure deficit turns out to be much smaller at the same time (c.f. Figure 6). Based on the analysis results, it appears that the model physics employed in the current 4DVAR analysis method could at most be applicable to a horizontal resolution of about 100 m. For finer horizontal resolution, the physics may break down, giving rise to meteorologically unreasonable analysis field.

6. CONCLUSIONS

A tornado event at HKIA is analyzed in this paper using 4DVAR analysis method as applied to the LIDAR data. One possibility for the occurrence of the tornado is the presence of the vorticity in the vertical circulation associated with a gust front. The analyzed wind and pressure fields appear reasonable using a horizontal resolution of 100 m.

This paper presents the preliminary analysis of the gustnado at its climax. Further studies would need to be carried out to analyze the causes for the occurrence of this tornado. This may be carried out through two approaches:

(a) The LIDAR data throughout the life cycle of the gustnado would be analyzed by, for instance, 4DVAR method in order to see the dynamic and

thermodynamic fields associated with the gustnado, from its initial occurrence, development and eventual weakening. However, there may be limitation in the analysis of the gustnado using this method because the LIDAR PPI scans have low elevation angles only (with the largest elevation angle being 4.5 degrees from the horizon) and thus it may not be possible to completely resolve the vertical circulation associated with the gust front and the gustnado.

(b) The weather process would further be analyzed using the data from the Terminal Doppler Weather Radar at the Hong Kong International Airport. This radar scans at far larger number of elevation angles above the horizon and it may thus provide useful data about the vertical circulation, such as the upward motion responsible for tilting the vorticity across the gust front. The radar data may be analyzed by using Ground-Based Velocity Track Display (GBVTD) method, which has been successfully applied to the analysis of another tornado case at the airport.

REFERENCES

[1] Yu, F., P.W. Chan, 2009: Four Dimensional Variational (4DVAR) Analysis of the Wind Field Based on Doppler LIDAR Data, *Fourth Symposium on Lidar Atmospheric Applications,* Phoenix, U.S.A., 11 - 16 January 2009.

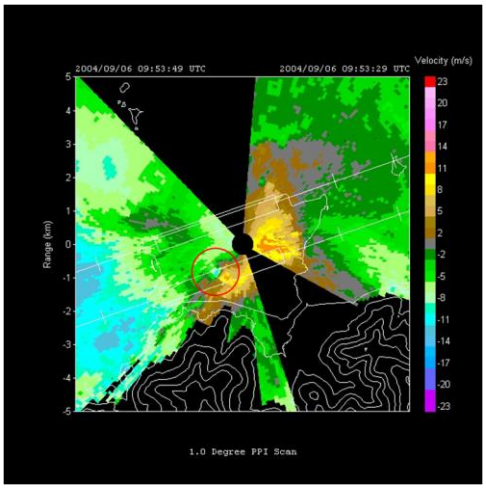

Figure 1 The LIDAR's 1-degree PPI scan image at the climax of the tornado at about 09:54 UTC, 6 September 2004.

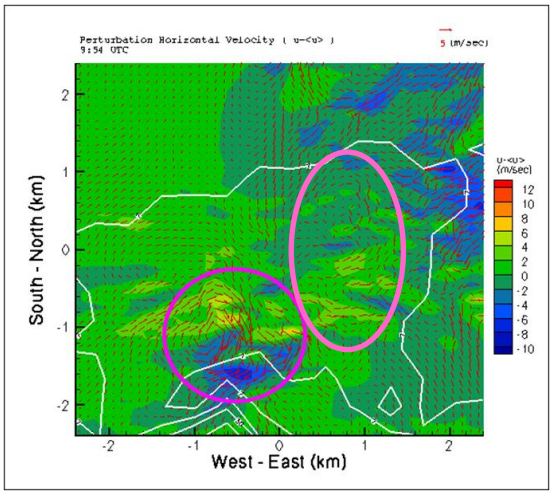

Figure 2 4DVAR-analyzed horizontal wind vectors (as arrows) and perturbation horizontal velocities (u - <u>, in colour contours) at a height of 200 m above sea level. Locations of small-scale cyclones and anticyclones are enclosed in pink ellipses.

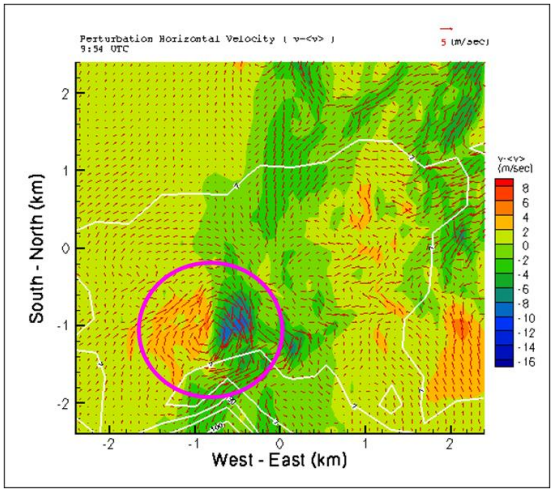

Figure 3 4DVAR-analyzed horizontal wind vectors (as arrows) and perturbation horizontal velocities (v - <v>, in colour contours) at a height of 200 m above sea level.

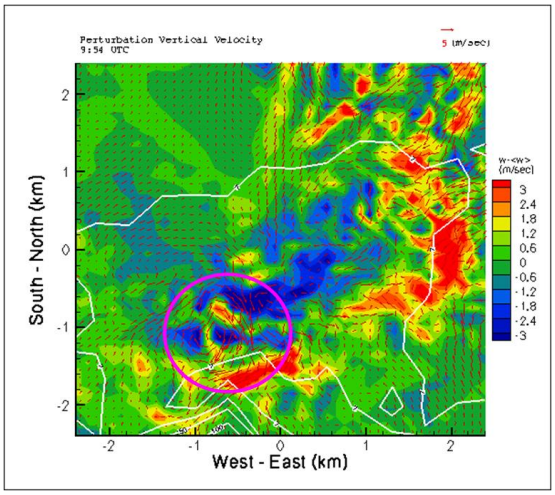

Figure 4 4DVAR-analyzed perturbation vertical velocity with the horizontal wind vectors overlaid.

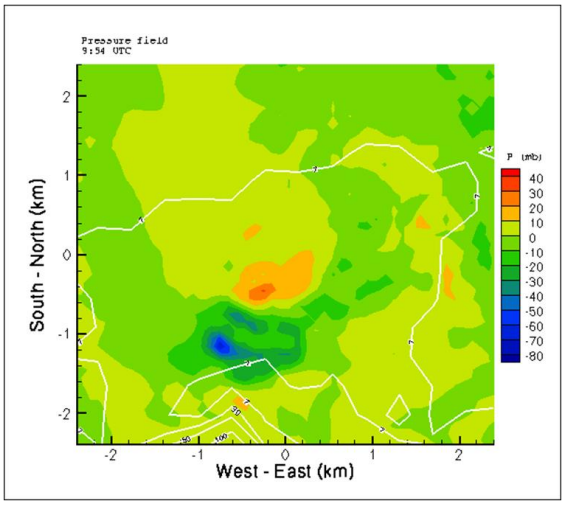

Figure 5 4DVAR-analyzed perturbation pressure field at 200 m above sea level.

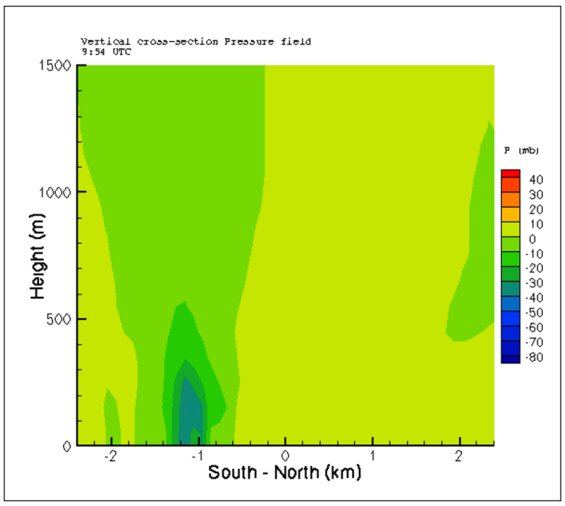

Figure 6 Vertical cross section of the pressure field along north-south direction at the core of the pressure deficit.

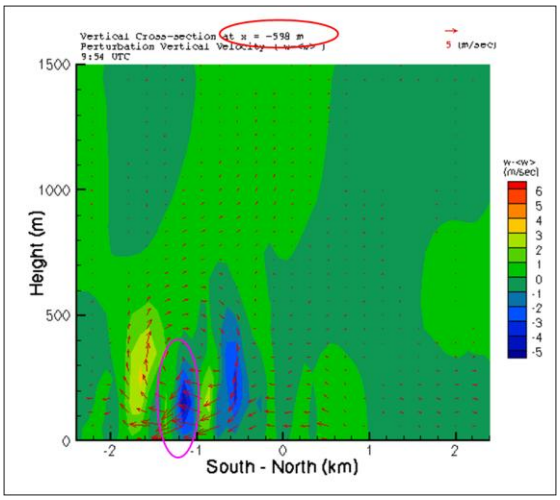

Figure 7 Vertical cross section of the perturbation vertical velocity at x = -598m along north-south direction from LIDAR.

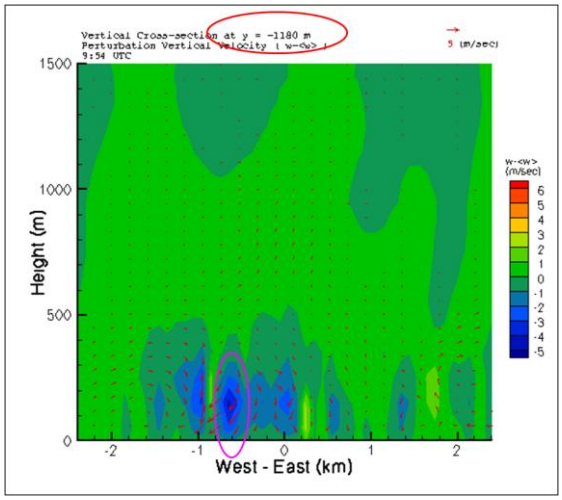

Figure 8 Vertical cross section of the perturbation vertical velocity at y = -1180m along east-west direction from LIDAR.

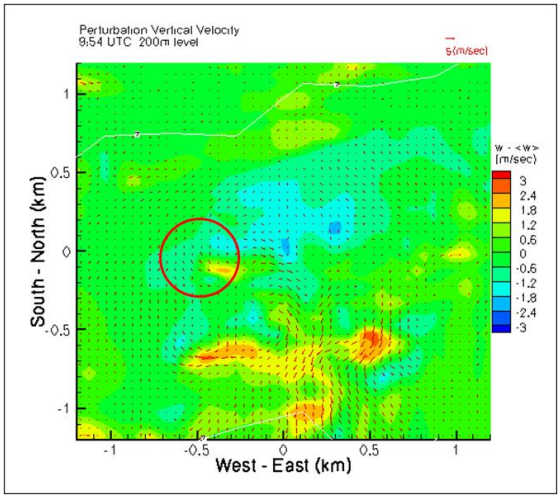

Figure 9 Perturbation vertical velocity using 50m horizontal resolution 4DVAR analysis.

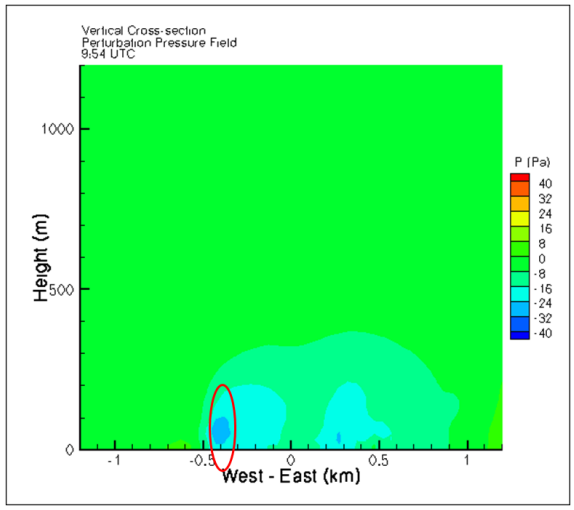

Figure 10 Vertical cross section of the pressure field along east-west direction at the core of the pressure deficit using 50m horizontal resolution 4DVAR analysis.